Oral presentation | CS Code-sharing session：【CS.7】 Code-sharing Session of 4.5 & 17

Wed. Sep 20, 2023 1:00 PM - 6:45 PM JST | Wed. Sep 20, 2023 4:00 AM - 9:45 AM UTC | A602 (KJ Hall)

[20p-A602-1~16] CS.7 Code-sharing Session of 4.5 & 17

Ryo Kitaura(NIMS), Kazunari Matsuda(Kyoto Univ.), Yuhei Miyauchi(Kyoto Univ.), Yuichiro K. Kato(RIKEN)

English Presentation

1:00 PM - 1:30 PM JST | 4:00 AM - 4:30 AM UTC

[20p-A602-1] [JSAP-Optica Joint Symposia 2023 Invited Talk] Direct observation of electronic structures in atomically thin flakes by using micro-focused angle-resolved photoemission spectroscopy

○Masato Sakano[1] (1.The Univ. of Tokyo)

English Presentation

1:30 PM - 1:45 PM JST | 4:30 AM - 4:45 AM UTC

[20p-A602-2] Direct imaging of valley-polarized excitons in 2D semiconductors

David R. Bacon[1], ○(D)Xing Zhu[1], Vivek Pareek[1], Kenji Watanabe[2], Takashi Taniguchi[2], Michael K. L. Man[1], Julien Madeo[1], Keshav M. Dani[1] (1.Femtosecond Spectroscopy Unit, OIST, 2.National Institute for Materials Science)

English Presentation

1:45 PM - 2:00 PM JST | 4:45 AM - 5:00 AM UTC

[20p-A602-3] Extreme UV photoemission electron microscopy imaging of moiré ferroelectricity in a twisted hBN heterostructure

○(P)Jacques Gabriel Hawecker[1], Prajakta Kokate[1], Risa Hocking[2], Kenji Watanabe[3], Takashi Taniguchi[3], Julien Madeo[1], Michael K. L. Man[1], Andrew J. Mannix[2], Keshav M. Dani[1] (1.OIST, 2.Stanford University, 3.NIMS)

English Presentation

2:15 PM - 2:45 PM JST | 5:15 AM - 5:45 AM UTC

[20p-A602-4] [JSAP-Optica Joint Symposia 2023 Invited Talk] Synthesis of wafer-scaled single-crystal 2D layered materials via chemical vapor deposition

○Ki Kang Kim[1] (1.Sungkyunkwan Univ.)

English Presentation

2:45 PM - 3:00 PM JST | 5:45 AM - 6:00 AM UTC

[20p-A602-5] Tracking Optical Properties During Atomic Substitution Process from $MoSe_2$ to Janus MoSeS

○Hiroo Suzuki[1], Masaaki Misawa[2], Yingzhe Wang[1], Kenji Tsuruta[1], Yasuhiko Hayashi[1] (1.Okayama Univ., 2.FIT)

Presentation by Applicant for JSAP Young Scientists Presentation Award English Presentation

3:00 PM - 3:15 PM JST | 6:00 AM - 6:15 AM UTC

[20p-A602-6] Strain Modulation to Moiré Superlattices in Transition Metal Dichalcogenide van der Waals Heterostructures

○(D)Hao Ou[1], Koshi Oi[1], Rei Usami[1], Takahiko Endo[2], Keisuke Shinokita[3], Kazunari Matsuda[3], Yasumitsu Miyata[2], Jiang Pu[4], Taishi Takenobu[1] (1.Nagoya Univ., 2.Tokyo Metropolitan Univ., 3.Kyoto Univ., 4.Tokyo Inst. of Tech.)

English Presentation

3:15 PM - 3:30 PM JST | 6:15 AM - 6:30 AM UTC

[20p-A602-7] Pd Decoration at Vertical Edge of MoS_2 for Enhanced NO_2 Sensitivity: A DFT Study

○(DC)ADITYA KUSHWAHA[1], NEERAJ GOEL[1] (1.NEATJI SUBHAS UNIVERSITY OF TECHNOLOGY, DWARKA, SECTOR 3, DELHI)

English Presentation

3:45 PM - 4:15 PM JST | 6:45 AM - 7:15 AM UTC

[20p-A602-8] [JSAP-Optica Joint Symposia 2023 Invited Talk] Upconversion electroluminescence in van der Waals tunnel diodes

○Goki Eda[1] (1.National Univ. of Singapore)

English Presentation

4:15 PM - 4:30 PM JST | 7:15 AM - 7:30 AM UTC

[20p-A602-9] Elucidating Upconversion Photoluminescence Mechanisms in Air-Suspended Single-Walled Carbon Nanotubes

○Daichi Kozawa[1,2,3], Yuichiro K. Kato[1,2] (1.RAP, RIKEN, 2.CPR, RIKEN, 3.MANA, NIMS)

English Presentation

4:30 PM - 4:45 PM JST | 7:30 AM - 7:45 AM UTC

[20p-A602-10] Determination of in- and out-of-plane complex refractive index spectra of single-chirality carbon nanotube membranes

○Hengkai Wu[1], Taishi Nishihara[1], Akira Takakura[1], Kazunari Matsuda[1], Takeshi Tanaka[2], Hiromichi Kataura[2], Yuhei Miyauchi[1] (1.Kyoto Univ. IAE, 2.AIST)

English Presentation

4:45 PM - 5:00 PM JST | 7:45 AM - 8:00 AM UTC

[20p-A602-11] Changing from diffusive to superdiffusive transport in carbon nanotube networks via nematic order control

○(PC)Filchito Bagsican[1,2], Michael Wais[3,4], Natsumi Komatsu[5,6], Weilu Gao[7], Kazunori Serita[1], Hironaru Murakami[1], Karsten Held[4], Iwao Kawayama[8,1], Junichiro Kono[5,1,3], Marco Battiato[3], Masayoshi Tonouchi[1] (1.Osaka Univ., 2.FSU, OIST, 3.NTU, 4.TU Wien, 5.Rice Univ., 6.UC Berkeley, 7.Univ. of Utah, 8.Kyoto Univ.)

Presentation by Applicant for JSAP Young Scientists Presentation Award English Presentation

5:00 PM - 5:15 PM JST | 8:00 AM - 8:15 AM UTC

[20p-A602-12] Plasmonic rectification effect in an asymmetric periodically gated graphene field effect transistor for THz detection

○Chao Tang[1,2], Hironobu Seki[1,3], Koichi Tamura[1,3], Shinnosuke Uchigasaki[1,3], Hirokazu Fukidome[1], Yuma Takida[4], Hiroaki Minamide[4], Akira Satou[1], Taiichi Otsuji[1] (1.RIEC, Tohoku Univ., 2.FRIS, Tohoku Univ., 3.School of Eng. Tohoku Univ., 4.RAP, RIKEN)

English Presentation

5:30 PM - 6:00 PM JST | 8:30 AM - 9:00 AM UTC

[20p-A602-13] [JSAP-Optica Joint Symposia 2023 Invited Talk] Moiré excitonic states in a twisted $WSe_2/MoSe_2$ heterobilayer

○Keisuke Shinokita[1] (1.IAE, Kyoto Univ.)

English Presentation

6:00 PM - 6:15 PM JST | 9:00 AM - 9:15 AM UTC

[20p-A602-14] Remote charge modulation effect of monolayer MoS_2 using periodically polarization-inverted structure and hBN spacer layer

Rong Kaippeng[1], Ryosuke Noro[2], Hayato Nishigaki[2], MIngda Ding[2], Yao Yao[2], Taiki Inoue[2], Ryuji Katayama[2], Yoshihiro Kobayashi[2], Kazunari Matsuda[3], ○Shinichiro Mouri[1] (1.Ritsumeikan Univ., 2.Osaka Univ., 3.Kyoto Univ.)

Presentation by Applicant for JSAP Young Scientists Presentation Award English Presentation

6:15 PM - 6:30 PM JST | 9:15 AM - 9:30 AM UTC

[20p-A602-15] Observation of quantum coherence of a single moiré exciton in nano-fabricated twisted $MoSe_2/WSe_2$ heterobilayers

○(D)Wang Haonan[1], Heejun Kim[1], Duanfei Dong[1], Keisuke Shinokita[1], Kenji Watanabe[2], Takashi Taniguchi[3], Kazunari Matsuda[1] (1.Institute of Advanced Energy, Kyoto Univ., 2.Research Center for Electronic and Optical Materials, NIMS, 3.Research Center for Materials Nanoarchitectonics, NIMS)

English Presentation

6:30 PM - 6:45 PM JST | 9:30 AM - 9:45 AM UTC

[20p-A602-16] Chemically-tailored semiconductor moiré superlattices

○Wenjin Zhang[1], Zheng Liu[2], Hiroshi Nakajo[3,4], Soma Aoki[3], Haonan Wan[5], Yanlin Wang[5], Yanlin Gao[6], Mina Maruyama[6], Takuto Kawakami[7], Yasuyuki Makino[1], Masahiko Kaneda[1], Tongmin Chen[8], Kohei Aso[8], Tomoya Ogawa[6,1], Takahiko Endo[1], Yusuke Nakanishi[1], Kenji Watanabe[9], Takashi Taniguchi[9], Yoshifumi Oshima[8], Yukiko Yamada-Takamura[8], Mikito Koshino[7], Susumu Okada[6], Kazunari Matsuda[5], Toshiaki Kato[3], Yasumitsu Miyata[1] (1.Tokyo Metropolitan Uni., 2.AIST, 3.Tohoku Uni, 4.KOKUSAI ELECTRIC, 5.Kyoto Uni, 6.Uni. of Tsukuba, 7.Osaka Uni., 8.JAIST, 9.NIMS)

Direct observation of electronic structures in atomically thin flakes by using micro-focused angle-resolved photoemission spectroscopy

QPEC and Dept. of Appl. Phys, The Univ. of Tokyo, **Masato Sakano**

E-mail: Sakano@ap.t.u-tokyo.ac.jp

The physical properties of atomically-thin, two-dimensional (2D) materials drastically change as the number of layers decreases towards the monolayer limit. The quantization of band dispersions along the stacking direction, as well as the reduction of symmetry compared to the infinite bulk crystal, can significantly modify the electronic structures of 2D materials, resulting in peculiar physical phenomena.

WTe_2, the material we focused on in our study, is a representative example. Bulk WTe_2 is a charge-compensated polar semimetal [1] predicted to be an inversion-symmetry-broken type-II Weyl semimetal [2]. In contrast, mono- and bi-layer WTe_2 are known as insulators with small band gaps [3-5]. In terms of structural symmetry, although monolayer WTe_2 is centrosymmetric, the stacking order of layers breaks the inversion symmetry in few-layer WTe_2, leading to unique phenomena related to the Berry-curvature dipole [4-8]. The aforementioned studies on thin-flake WTe_2 have primarily proceeded by comparing the transport properties of micro-devices with band calculations. Due to the limited size (typically ~0.01 mm) and volume of the samples, as well as the difficulty in handling them, many of the physical property measurements established in bulk systems are not applicable. Nevertheless, the precise investigation of the electronic structure is extremely important, especially considering that the properties related to Berry-curvature are determined by the electronic band dispersions in reciprocal space.

In our study, we used micro-focused laser angle-resolved photoemission spectroscopy (ARPES) in combination with a 2D materials manufacturing system (2DMMS) [9], which can freely stack atomic layers using image recognition, machine learning, and robotic assembly. We developed an efficient procedure for investigating the band dispersions of atomically thin micro-flakes[10]. We prepared 2D WTe_2 flake samples for ARPES by using graphite/hBN as a substrate and encapsulating them with graphene. We successfully observed the thickness-dependent band structures of these atomically thin WTe_2 flakes. This clearly revealed an insulator–semimetal transition occurring between the 2- and 3-layer states, as well as a striking even–odd effect in the layer-number dependence of the spin-band splitting [11].

The sample preparation procedure we have developed is adaptable to van der Waals heterostructures with complex structures. In the latter part of the presentation, I will introduce recent studies where we have observed the electronic structures in twisted materials with complex structures.

[1] M. N. Ali, *et al*., Nature **514**, 205, (2014).
[2] A. A. Soluyanov, *et al*., Nature **527**, 495 (2015).
[3] Z. Fei, *et al*., Nat. Phys. **13**, 677 (2017).
[4] Z. Fei, *et al*., Nature **560**, 336 (2018).
[5] I. Cucchi, *et al*., Nano Lett. **19**, 554 (2019).
[6] K. Kang, *et al*., Nat. Mater. **18**, 324 (2019).
[7] H. Wang and X. Qian, npj Comput. Mater. **5**, 119 (2019).
[8] J. Xiao, *et al*., Nat. Phys. **16**, 1028 (2020).
[9] S. Masubuchi, *et al*., Nat. COmmun. **9**, 1413 (2018).
[10] S. Masubuchi*, M. Sakano*, Y. Tanaka* *et al*., Sci. Rep. **12**, 10936 (2022).
[11] M, Sakano*, Y. Tanaka*, S. Masubuchi* *et al*., Phys. Rev. Res. **4**, 023247 (2022).
(* equally contributed)

Direct imaging of valley-polarized excitons in 2D semiconductors

David R. Bacon[1†], Xing Zhu[1†], Vivek Pareek[1†], Kenji Watanabe[2], Takashi Taniguchi[2], Michael K. L. Man[1], Julien Madéo[1], and Keshav M. Dani[*1]

[1] Femtosecond Spectroscopy Unit, Okinawa Institute of Science and Technology Graduate University, Onna, Okinawa, Japan 904-0495

[2] National Institute for Materials Science, 1-1 Namiki, Tsukuba, Ibaraki, Japan 305-0044

*E-mail: kmdani@oist.jp

† These authors contributed equally to this work.

1. Introduction

The monolayer transition-metal dichalcogenides (TMDCs), lacking inversion symmetry, allow the manipulation of excitonic states with valley degree of freedom through circularly polarized light [1-3]. However, with the complex landscape of exciton species in TMDCs, such as spin- or momentum- forbidden dark excitons, the valley depolarization mechanisms, which are of great importance for valleytronic applications, still lack clear understanding. Such measurements require direct access to the momentum and energy coordinate of constituent electrons and holes, but few experimental techniques provide such information. Meanwhile, time- and angle- resolved photoemission spectroscopy (TR-ARPES) has become a powerful tool to study excitons of 2D semiconductors in energy-momentum space [4-7]. In this talk, we focus on our momentum-resolved study on the valley-polarized excitons in monolayer WS_2 using TR-ARPES.

2. Experiments

We perform experiments on an exfoliated monolayer WS_2 stacked on an hBN buffer layer and a Si substrate, as plotted in Fig 1(a). The experimental setup, similar to that employed in our previous studies [4-6], consists of a home-built table-table beamline used to generate a 21.7eV XUV probe to photoemit the electrons from the sample. The electrons are further analyzed by a momentum microscope to map the 3D band-structure of the material (E, k_x, k_y).

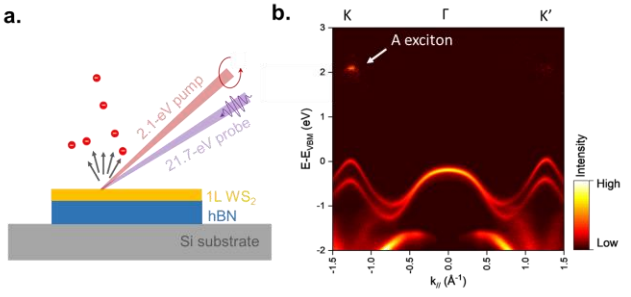

Figure 1. (a) Experimental schematic of the sample geometry with circularly polarized optical pump and XUV probe. (b) Energy-momentum cut from K to Γ, and to K'. The plot is taken at 0ps upon the photoexcitation.

To create valley-polarized excitons, a circularly polarized pump pulse resonant with the WS_2 A exciton (2.1eV) is used to excite the sample. A-excitons are initially selectively photoexcited in the K valley, as shown in Figure 1(b). The following ultrafast depopulation and depolarization of bright excitons are further tracked in these time-resolved measurements.

3. Conclusions

Valley-polarized excitons in monolayer WS_2 are imaged in momentum and energy space using TR-ARPES. This study reveals the dynamics of the depolarization and the interplay between bright and dark excitons.

Acknowledgements

This work was supported in part by JSPS Kakenhi grant number 21H01020. Funding was also provided in part by the Femtosecond Spectroscopy Unit of the Okinawa Institute of Science and Technology Graduate University. We thank the OIST engineering support section for their support.

References

[1] W. Yao, D. Xiao and Q. Niu, Phys. Rev. B Condens. Matter **77** (2008) 235406.

[2] D. Xiao, G.-B. Liu, W. Feng, X. Xu and W. Yao, Phys. Rev. Lett. **108** (2012) 196802.

[3] S. A. Vitale, D. Nezich, J. O. Varghese, P. Kim, N. Gedik, P. Jarillo-Herrero, D. Xiao and M. Rothschild, Small. **14** (2018) e1801483.

[4] J. Madéo, M. K. L. Man, C. Sahoo, M. Campbell, V. Pareek, E. L. Wong, A. Al-Mahboob, N. S. Chan, A. Karmakar, B. M. K. Mariserla, X. Li, T. F. Heinz, T. Cao and K. M. Dani, Science **370** (2020) 1199.

[5] M. K. L. Man, J. Madéo, C. Sahoo, K. Xie, M. Campbell, V. Pareek, A. Karmakar, E. L. Wong, A. Al-Mahboob, N. S. Chan, D. R. Bacon, X. Zhu, M. M. M. Abdelrasoul, X. Li, T. F. Heinz, F. H. da Jornada, T. Cao and K. M. Dani, Science Advances **7** (2021) eabg0192.

[6] O. Karni, E. Barré, V. Pareek, J. D. Georgaras, M. K. L. Man, C. Sahoo, D. R. Bacon, X. Zhu, H. B. Ribeiro, A. L. O'Beirne, J. Hu, A. Al-Mahboob, M. M. M. Abdelrasoul, N. S. Chan, A. Karmakar, A. J. Winchester, B. Kim, K. Watanabe, T. Taniguchi, K. Barmak, J. Madéo, F. H. da Jornada, T. F. Heinz and K. M. Dani, Nature **603** (2022) 247.

[7] D. Schmitt, J. P. Bange, W. Bennecke, A. AlMutairi, G. Meneghini, K. Watanabe, T. Taniguchi, D. Steil, D. R. Luke, R. T. Weitz, S. Steil, G. S. M. Jansen, S. Brem, E. Malic, S. Hofmann, M. Reutzel and S. Mathias, Nature **608** (2022) 499.

Extreme UV photoemission electron microscopy imaging of moiré ferroelectricity in a twisted hBN heterostructure

Jacques Hawecker. [1], Prajakta Kokate. [1], Risa Hocking[2], Kenji Watanabe[3], Takashi Taniguchi[3] Julien Madéo[1], Michael K. L. Man1[1], Andrew J. Mannix[2], Keshav M. Dani[1]
[1] Femtosecond Spectroscopy Unit, Okinawa Institute of Science and Technology Graduate University, Onna-son; Okinawa, 904-0495 Japan
[2]Department of Materials Science and Engineering, Stanford University,Stanford, CA 94305, USA.
[3] Research Center for Functional Materials, National Institute for Materials Science, Tsukuba, Japan
E-mail: Jacques.Hawecker@oist.jp

1. Introduction

Photoemission electron microscopy (PEEM) is a powerful technique allowing to map real space electronic distribution at different energies, providing high resolution imaging and spectroscopic information of a sample's surface [1,2]. However, typical table-top light source coupled with this technique do not allow for: 1) Extreme UV (XUV) energies to access larger Brillouin zones, all the valence bands and shallow core-levels (thus providing electronics and chemical information), 2) brightness required for nanoscale imaging and 3) time resolution to capture ultrafast dynamics. Recently, by bringing together Angle Resolved Photoemission (ARPES) and our ultrafast table-top based XUV source, we built a novel instrumentation capable of capturing the bandstructure of the material under optical excitation. This already provided important breakthrough in the field by providing momentum resolved visualizations of dark Xtons [3], excitonic wavefunctions in monolayer transition metal dichalcogenide [4] and in heterostructures [5]. However, to demonstrate nanometer-scale resolution XUV-PEEM imaging, one must overcome the large photon flux per area requirement and consequently space or sample charge effect. In this work, using another iteration of our light source coupled to our PEEM, we show imaging capability of resolving 2D moiré ferroelectric domain from a twisted hexagonal Boron Nitride (hBN).

2. Experimental setup & twisted hBN

Our XUV beamline is based on a tabletop Yb doped fiber amplifier laser system radiating ultrafast pulses of 1030nm operated a 1MHz. We generate the second harmonic (515nm) by using a LBO non critically phase matched crystal. The XUV (21.7eV) pulses are generated by high harmonic generation from our second harmonic focused in a Kr gas jet, similarly to our previous work [3]. To tightly focus the XUV beam on the sample, we use a synchrotron grade ellipsoidal mirror yielding a beam of ~40x10um. This beam is spectrally filtered by a combination of thin Al and Sn filters and then coupled into our ELMITEC SPELEEM.

The sample used to illustrate our beamline capabilities is a twisted hBN heterostructure. hBN is an important building block for 2D heterostructures due to its insulator properties, low levels of charge disorder, or its large flat terrasses. It has been shown recently that a twisted hBN/hBN interface can be engineered with out-of-plane ferroelectric polarization by breaking inversion symmetry (i.e., with AB stacking, twisted 60º from bulk AA' order). Adding a small twist between the layers creates a moiré pattern, each moiré unit cell has one up and one down domain [6–8]. In this work, we fabricate a twisted hBN heterostructure that shows ferroelectric domains. We investigate this heterostructure with our state-of-the-art PEEM coupled to a tightly focused XUV beam in combination of other light sources to do time resolved measurement.

We have succeeded in accurately imaging the ferroelectric domains, in real space (see Figure 1) using our home built MHz XUV light source. Furthermore, from photoelectron spectroscopy (PES), we identified the band alignment within the ferroelectric domains. Finally, we captured the full Brillouin zone of our hBN structure using XUV-ARPES.

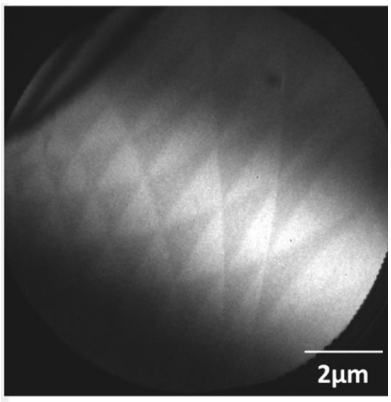

Figure 1 XUV PEEM imaging of the gamma valley valence band top (integration of 1eV) from our twisted hBN heterostructure.

Acknowledgements

We would like to express sincere thanks to all the contributors to the symposia for their cooperation.

References

[1] M. K. L. Man et al., Nature Nanotech **12**, 1 (2017).
[2] T. A. S. Doherty et al., Nature **580**, 7803 (2020).
[3] J. Madéo et al., Science **370**, 1199 (2020).
[4] M. K. L. Man et al., Sci. Adv. **7**, eabg0192 (2021).
[5] O. Karni et al., Nature **603**, 247 (2022).
[6] C. R. Woods, et al., Nat Commun **12**, 1 (2021).
[7] M. Vizner Stern et al., Science **372**, 1462 (2021).
[8] K. Yasuda et al., Science **372**, 1458 (2021).

Synthesis of wafer-scaled single-crystal 2D layered materials via chemical vapor deposition

Ki Kang Kim, Department of Energy Science, Sungkyunkwan University

E-mail: kikangkim@skku.edu

Two-dimensional (2D) materials including graphene, hexagonal boron nitride, and transition metal dichalcogenide have been paid attentions due to unusual intrinsic physical and chemical properties such as high exciton binding energy and large magnetic resistance. Such unusual properties allow unprecedented applications. To realize the intrinsic material properties and industrial applications, wafer-scaled single-crystal 2D films are highly required. Here, I present the recent progress of single-crystal growth for 2D van der Waals materials in a wafer scale via the self-collimation on liquid substrate and the epitaxial growth on self- atomic sawtooth surface. The detailed growth mechanism is discussed accordingly.

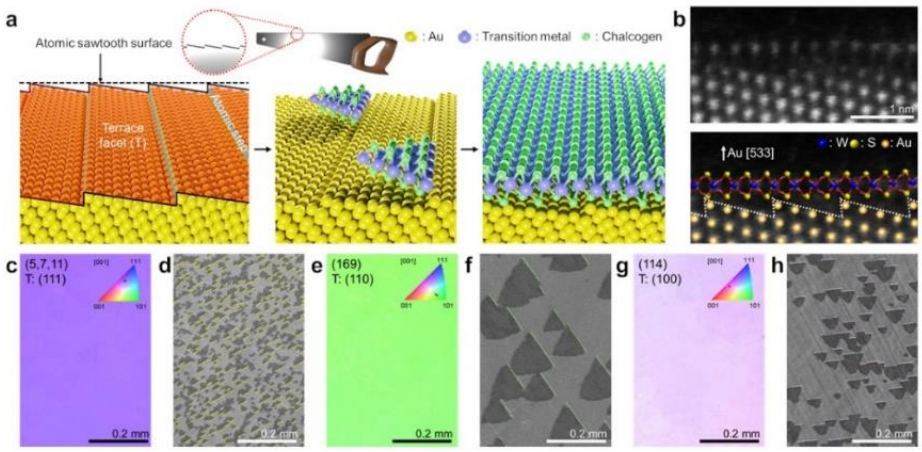

Fig 1. Growth of single-crystal WS_2 on atomic sawtooth Au surface. a) Schematic illustration of WS_2 film grown via an atomic sawtooth Au surface. b) Cross-sectional ADF-STEM image and the corresponding ball-and-stick model of as-grown WS_2 on an atomic sawtooth Au (533) surface. c,e,g) EBSD IPF maps and d,f,h) SEM images of coherently aligned WS_2 grains on Au (5,7,11), (169), and (114) with respective (111), (110), and (100) terrace facets.

Tracking Optical Properties During Atomic Substitution Process from $MoSe_2$ to Janus MoSeS

Hiroo Suzuki [1], Masaaki Misawa [2], Yingzhe Wang [1], Kenji Tsuruta [1], Yasuhiko Hayashi [1]

[1] Okayama University, [2] Fukuoka Institute of Technology
E-mail: hiroo.suzuki@okayama-u.ac.jp

1. Introduction

Janus transition metal dichloride (TMDC) is a TMDC with two different chalcogenide elements on the upper and lower surfaces. This special structure is reported to break the out-of-plane symmetry of the monolayer TMDC and produce out-of-plane polarization. This is expected to lead to the development of new electronic properties, such as Rashba spin splitting and piezoelectricity. There have been several reports on the synthesis of Janus TMDCs, and in recent years, the use of chalcogen spices containing H_2 plasma for atomic substitution on the surface of TMDC has attracted attention since Janus TMDCs can be generated at room temperature [1,2]. However, the generation process of Janus TMDCs with this method has not been well understood. In addition, the physical properties in the intermediate state between TMDC and Janus TMDC have also not been clarified, although the control of the intermediate state is important for tuning the physical properties of Janus TMDCs. Thus, elucidating the intermediate partially substituted Janus (PSJ) state between $MoSe_2$ and Janus MoSeS state is essential for understanding the synthesis dynamics and tuning the electrical properties of TMDCs.

2. Results

In this study, Janus MoSeS was produced using the S-containing H_2 plasma (H_2/S-plasma) with surface atomic substitution of monolayer $MoSe_2$. As such, the repeated power-controlled plasma treatment enabled the investigation of the intermediated PSJ state between $MoSe_2$ and Janus MoSeS. Moreover, the gradual atomic transition from $MoSe_2$ to Janus MoSeS was observed using X-ray photoelectron spectroscopy. The scanning transmission microscopy observation successfully revealed the PSJ structure at the atomic scale. Notably, we discovered the newly emerged Raman mode (peak X) specific to the PSJ structure during H_2/S plasma treatment (Fig. 1), which was reproducible with density functional theory (DFT) calculations. The photoluminescence (PL) presented the bandgap energy modulation with the S substitution ratio, which was consistent with the DFT calculations. Furthermore, we detected anomalous transition discontinuities of PL spectra in the early atomic-substitution stage, which could not be fully explained by the DFT calculations. We then proposed the possible model of the discontinuous PL transition, focusing on the competition between the domain size of Janus MoSeS formed in the PSJ structure and the exciton Bohr radius [3].

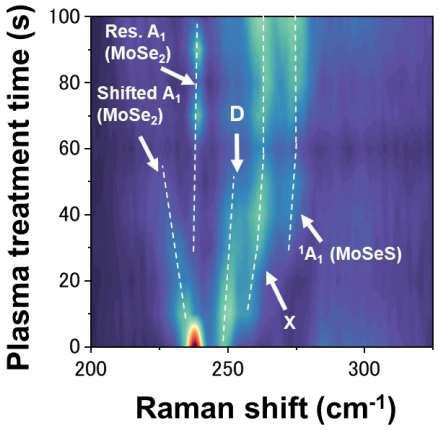

Figure 1: Mapping of Raman spectra with H_2/S-plasma treatment time.

3. Conclusions

The elucidation of the intermediate PSJ state between $MoSe_2$ and Janus MoSeS provides a deep understanding of the atomic substitution process during the synthesis of Janus TMDCs. The Raman peaks appearing in the PSJ state will help to characterize the degree of atomic substitution during synthesis. In addition, the control of this PSJ state will be significantly beneficial for tuning the properties of the Janus TMDC, such as its band gap, piezoelectricity, and spin splitting. Furthermore, the tunability of these properties will significantly contribute to realizing high-performance electronic devices based on Janus TMDCs. Further investigation of the electronic state of PSJ in relation to the possible effects such as the competition between the domain size of Janus MoSeS and the exciton Bohr radius will be essential for achieving a complete understanding of the phenomena emergent in the PSJ state.

Acknowledgements

We would like to thank Dr. C. Nakano (Okayama Univ.) for helping with XPS data acquisition and analysis, Ms. Y. Liu for engaging in experimental data acquisition, and the Foundation for the Promotion of Material Science and Technology of Japan (MST) for contract analysis.

References

[1] D. Trivedi *et al.*, Adv. Mater. **32**, 2006320 (2020).

[2] Y. Guo *et al.*, PNAS **118**, e2106124118 (2021).

[3] H. Suzuki *et al.*, Nano Lett **23**. 4533 (2023).

Strain Modulation to Moiré Superlattices in Transition Metal Dichalcogenide van er Waals Heterostructures

Hao Ou[1], Koshi Oi[1], Rei Usami[1], Takahiko Endo[2], Keisuke Shinokita[3], Kazunari Matsuda[3], Yasumitsu Miyata[2], Jiang Pu[4], Taishi Takenobu[1]

[1]Department of Applied Physics, Nagoya University, [2]Department of Physics, Tokyo Metropolitan University, [3]Institute of Advanced Energy, Kyoto University, [4]Department of Physics, Tokyo Institute of Technology
E-mail: takenobu@nagoya-u.jp

1. Introduction

The existence of moiré pattern in van der Waals heterostructures brings highly tunable electronic structure and rich physical properties[1-2], which opens the possibility of using the moiré heterostructures to simulate quantum phenomena in condensed-matter systems [3]. The controllability to moiré heterostructure greatly depends on the symmetry and period of moiré pattern. Currently the pattern is determined by material choice and twist angle. Meanwhile, there have been several studies showing that the heterostrain (that is, the strain state difference between monolayers) also significantly modulates the moiré pattern and corresponding physical properties of heterostructure [4-5]. However, experimental realization of controlled heterostrain introduction remains challenging. Here, we report the observation of continuous modulation of moiré pattern by uniaxial strain application.

2. Results and Discussion

We fabricated twisted bilayer WSe_2 on flexible polyethylene naphthalate (PEN) substrates using dry transfer method (Fig. 1a). We used exfoliated hBN flake to pick up two WSe_2 monolayers with a twist angle. Then flipped the whole stack and transferred it onto PEN substrate. To investigate the relationship between heterostrain and twist angle, we fabricated samples with different twist angles. We used piezoresponse force microscopy (PFM) to directly resolve the moiré pattern [6] (Fig. 1a). Clear moiré patterns were observed (Figs. 1b-d), indicating the effectiveness of the proposed sample structure and fabrication method.

We then bent the PEN substrate continuously by mounting it on metallic molds with different surface curvatures. Because of the weakness of van der Waals interaction between two monolayers of WSe_2, heterostrain emerges. We observed the variation of moiré patterns in samples with a variety of twist angles. For sample whose twist angle is close to 0°, we observed a macroscopic shift and distortion of moiré domain. For the sample with twist angle of ~1.3° (Fig. 1b-d), by designing the status of strain, we found a continuous transition of moiré pattern. More interestingly, the hexagonal pattern changes into rectangular shape, as indicated by angle variation and FFT images. The transition indicates that the preliminary three-fold symmetry of strain-free sample was effectively broken into nearly two-fold. The results above indicate that the proposed structure is able to introduce heterostrain intentionally and effectively. We expect such method is able to tune the geometry of moiré pattern on demand, which then leads to the change of related physical properties and phenomena.

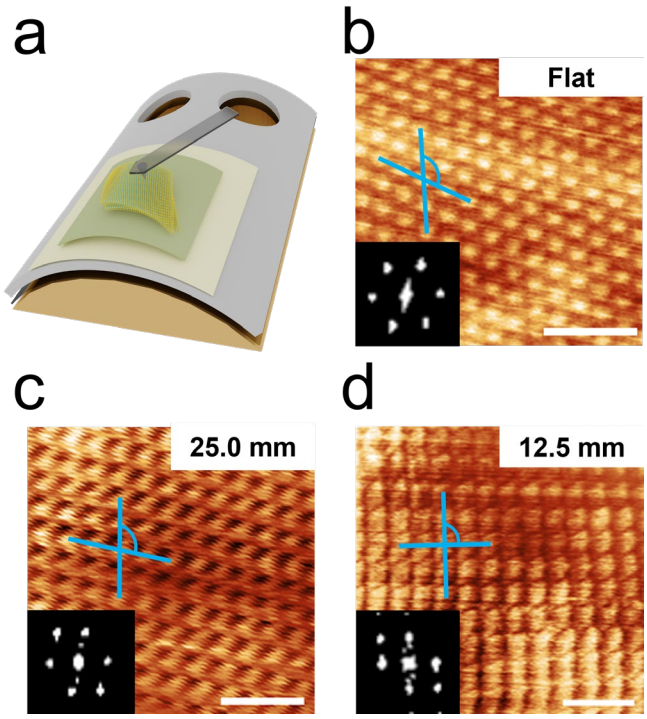

Fig.1 a. Schematic the device structure for uniaxial heterostrain application. b-d. Evolution of ~1.3° stacked bilayer WSe_2 when mold curvature was flat (b, 0% strain), 25.0 mm (c, 0.25%) and 12.5 mm (d, 0.5%), respectively. Insets show the corresponding FFT images. Scale bars: 50 nm.

3. Conclusions

In this study, we successfully observed the continuous transition of moiré patterns. We found a macroscope deformation of moiré domain for nearly 0° stacked bilayer. In ~1.3° stacked bilayer, a gradual transition of moiré pattern from hexagonal shape to rectangles was observed. The results prove the reliability of the method to modify the properties of moiré heterostructures.

References

[1] Y. Cao, et al., Nature **556** (2018) 80.
[2] K. L. Seyler, et al., Nature, **567** (2019) 66.
[3] D. M. Kennes, et al., Nat. Phys. **17** (2021) 155.
[4] Z. Bi, et al., Phys. Rev. B **100** (2019) 035448.
[5] Y. Bai, et al., Nat. Mater. **19** (2020) 1068.
[6] L. J. McGilly et al., Nat. Nanotechnol. **15** (2020) 580.

Pd Decoration at Vertical Edge of MoS_2 for Enhanced NO_2 Sensitivity: A DFT Study

Aditya Kushwaha[1], Neeraj Goel[1]
[1]Department of Electronics and Communication Engineering, Netaji Subhas University of Technology, Delhi, India
E-mail: aditya.kushwaha.phd21@nsut.ac.in

1. Introduction

Gas sensors are vital for safety, air quality monitoring, industrial enhancement, and emission compliance [1]. NO_2, a harmful gas released from the burning of fossil fuels, poses health hazards and contributes to pollution. Decorating noble metals on 2D transition metal dichalcogenide (TMD) nanomaterial-based gas sensors provides benefits like enhanced sensitivity, selectivity, fast response, and so on [2]. In this work, density functional theory (DFT) study compared NO_2 sensing in pristine MoS_2, Pd decorated at basal plane of MoS_2 (Pd-B-MoS_2), and Pd decorated at vertical edge of MoS_2 (Pd-V-MoS_2). Pd nanoparticles (NPs) decoration (top site) induce catalytic oxidation by extracting electrons from MoS_2 through Fermi level disparities [3]. NO_2, an electron-repelling compound, withdraws electrons from Pd-NPs. The spillover effect in Pd-V-MoS_2 amplifies its sensing capabilities by offering additional reactive Mo sites [4]. Pd-V-MoS_2 showed higher NO_2 sensitivity than MoS_2 and Pd-B-MoS_2.

2. COMPUTATIONAL METHODS

This study utilized material studio software with the DMol^3 package for DFT calculations. Optimization is performed with a 5x5x1 k-point grid and a global cut-off radius of 4.9 Å. Convergence criteria are set at $1.0x10^{-5}$ Ha for energy, 0.002 Ha/Å, and 0.005 Å for maximum force, and maximum displacement. The Perdew-Burke-Ernzerh generalized gradient approximation (GGA-PBE) with the double numerical plus polarization (DNP) basis set was employed for the exchange-correlation term [5]. Grimme's method with DFT Semi-core Pseudopots (DSPP) was used for calculating adsorption energies.

3. Result and Discussion

Fig. 1 displays 3x3x1 supercell structures of pristine MoS_2, Pd-B-MoS_2, and Pd-V-MoS_2, and their bandgap calculations using DMol^3 package, yielded values are 1.655eV, 1.531eV, and 0.082eV, respectively. Fig. 2 shows the charge density difference (CDD) between NO_2 and sensing layer. According to Mulliken analysis, the total charge over NO_2 was -0.014e, -0.179e, and -0.224e for pristine MoS_2, Pd-B-MoS_2, and Pd-V-MoS_2, respectively. Pd-V-MoS_2 exhibited higher electron withdrawal, attributed to the spillover effect and the presence of more active sites in comparison to the other configurations. Moreover, fig. 2 represents the most stable configuration among the proposed structures. The adsorption energy (E_{ad}) was calculated using eq 1 [6]:

$$E_{ad} = E_{NO_2/System} - E_{System} - E_{NO_2} \quad (1)$$

where, $E_{NO_2/System}$, E_{System}, and E_{NO_2} are the total energies of the NO_2 adsorbed system, isolated system, and NO_2, respectively. E_{ad} values were -0.203 eV, -1.023 eV, and -2.914 eV for pristine MoS_2, Pd-B-MoS_2, and Pd-V-MoS_2, respectively. Therefore, the Pd-V-MoS_2 configuration exhibited lower adsorption energy.

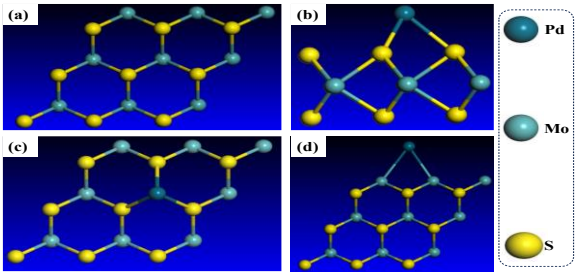

Fig. 1. Supercell of (a). Pristine MoS_2, (b and c). Pd-B-MoS_2, (d). Pd-V-MoS_2

Fig. 3 illustrates the sensing mechanism of the proposed structure. Pd nanoparticles (NPs) facilitate catalytic oxidation, extracting electrons from the MoS_2 monolayer due to the difference in Fermi levels. NO_2, being electron-withdrawing, withdraws electrons from Pd-NPs. The spillover effect in Pd-V-MoS_2 provides more active Mo sites, enhancing its sensing performance.

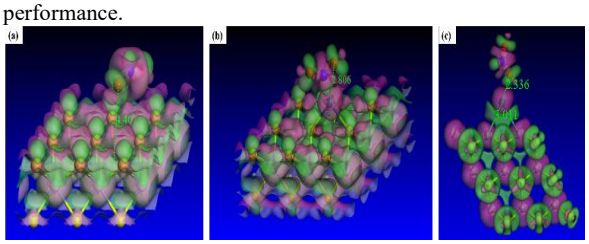

Fig. 2. CDD diagram of (a). Pristine MoS_2, (b). Pd-B-MoS_2, and (c). Pd-V-MoS_2. Green (Pink) color depicts electron accumulation(depletion)

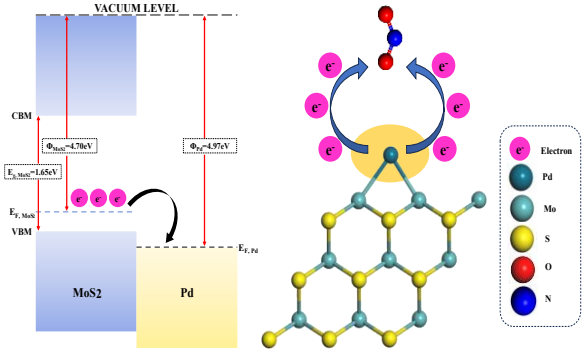

Fig. 3. Schematic diagram of sensing mechanism for the proposed structure

4. Conclusion

MoS_2 and Pd decorated MoS_2 structures are investigated for the sensing of NO_2 molecule using the DFT method. The result demonstrates that the Pd-V-MoS_2 is a potential candidate for NO_2 sensing among the proposed structures. This is due to the spillover effect and high active sites were available in vertical oriented MoS_2 structure.

REFERENCES

[1] Vardhan, Shalini, and Ritu Raj Singh. "Design, simulation and performance comparison of SoI rectangular waveguide and SMF for methane detection." In *Integrated Photonics Platforms II*, vol. 12148, pp. 107-112. SPIE, 2022.
[2] Wadhwa, Riya, Ashok Kumar, Ranjini Sarkar, Prajna Parimita Mohanty, Deepu Kumar, Sonia Deswal, Pradeep Kumar et al. "Pt Nanoparticles on Vertically Aligned Large-Area MoS2 Flakes for Selective H2 Sensing at Room Temperature." *ACS Applied Nano Materials* 6, no. 4 (2023): 2527-2537.
[3] Suh, Jun Min, Young-Seok Shim, Ki Chang Kwon, Jong-Myeong Jeon, Tae Hyung Lee, Mohammadreza Shokouhimehr, and Ho Won Jang. "Pd-and Au-decorated MoS2 gas sensors for enhanced selectivity." *Electronic Materials Letters* 15 (2019): 368-376.
[4] Cui, Hao, Dachang Chen, Ying Zhang, and Xiaoxing Zhang. "Dissolved gas analysis in transformer oil using Pd catalyst decorated MoSe2 monolayer: A first-principles theory." Sustainable Materials and Technologies 20 (2019): e00094.
[5] Xiao, Zhen, Wei Wu, Xiangwei Wu, and Youfa Zhang. "Adsorption of NO2 on monolayer MoS2 doped with Fe, Co, and Ni, Cu: A computational investigation." *Chemical Physics Letters* 755 (2020): 137768.
[6] Zhang, Dongzhi, Qi Li, Peng Li, Maosong Pang, and Yuwei Luo. "Fabrication of Pd-decorated MoSe 2 nanoflowers and density functional theory simulation toward ammonia sensing." *IEEE Electron Device Letters* 40, no. 4 (2019): 616-619.

Upconversion electroluminescence in van der Waals tunnel diodes

National University of Singapore[1], ○ Goki Eda[1]

E-mail: g.eda@nus.edu.sg

Plasmonic tunnel junctions comprising van der Waals semiconductor are an attractive platform where the interplay between inelastically tunneling electrons, surface plasmons, and excitons is expected to give rise to novel light emission phenomena. Here, we report observation of peculiar upconversion electroluminescene in van der Waals tunnel diodes comprising a monolayer transition metal dichalcogenide (TMD) in the electron tunneling pathway. The device exhibits bimodal electroluminescence with a broad low energy band and a narrow high energy band. Interestingly, the high energy emission, which is attributed to the TMD ground exciton, is found to turn on at applied biases significantly lower than the threshold defined by its emission energy whereas the low energy emission, which arises from plasmonic emission, strictly obeys the quantum cut-off (Figure 1). We examine several possible model and show that momentum-indirect excitation of high energy carriers enabled by inelastic electron tunneling is a key component enabling the apparent energy gain.

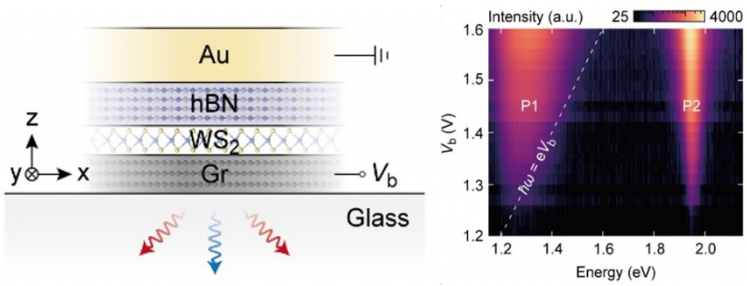

Figure 1. (left) Side-view schematic of a van der Waals tunnel diode device. (right) Emission intensity as a function of bias voltage and energy.

Elucidating Upconversion Photoluminescence Mechanisms in Air-Suspended Single-Walled Carbon Nanotubes

Daichi Kozawa[1,2,3], Yuichiro K. Kato [1,2]

[1] RIKEN Center for Advanced Photonics, [2] RIKEN Cluster for Pioneering Research,
[3] MANA, National Institute for Materials Science
E-mail: kozawa.daichi@nims.go.jp

Upconversion photoluminescence is the transformative process of lower energy photons into higher energy counterparts and holds intriguing potential for both fundamental science and advanced applications. This process is not only scientifically fascinating but also pivotal for sectors such as telecommunications, photonics, and renewable energy. The ability to perform upconversion in the near-infrared region could introduce new photonic devices, invigorate data transmission technologies, and enrich renewable energy fields.

An exceptional candidate to study and harness near-infrared upconversion is single-walled carbon nanotubes (SWNTs) [1]. The unique structure and distinct optical properties of SWNTs make them suitable platforms to investigate light-matter interactions. Their attractiveness is amplified by tightly bound excitons and strong exciton-phonon interactions inherent to these one-dimensional nanostructures. The ability of SWNTs to emit photons within the telecom band underscores their versatility across a broad range of potential applications. [2].

Despite the significant attention given to SWNTs, the study of upconversion photoluminescence (UCPL) within these nanostructures leaves many questions unanswered and presents numerous technical challenges. For instance, while a general understanding of the phonon-mediated upconversion process is available, there is still a lack of clarity surrounding the specific phonon modes and energies involved. Furthermore, the precise influences of exciton-phonon scattering, temperature, and different SWNT chiralities on upconversion efficiency remain areas to be further explored.

In this study, we elucidate the high-efficiency UCPL in air-suspended single-walled carbon nanotubes (SWNTs). UCPL is detected even in individual SWNTs despite the sizeable energy separation between the emission energy and excitation energy. We conduct power dependence of UCPL intensity and observe linear response, ruling out two-photon excitation as an upconversion source. Our exhaustive exploration of UCPL spectra across various chiralities highlights the universal presence of this upconversion process and energy separation dependence of UCPL intensity. In conducting upconversion photoluminescence excitation (UCPLE) spectroscopy across a broad range of energy separations, we discern UCPLE peaks as sidebands of *K*-momentum dark excitons where specific phonon modes at the K point are involved [3]. The high efficiency of the upconversion process can be attributed to the one-phonon process and the abundance of low-energy phonons. To better interpret these findings, we develop a physical model of exciton-phonon scattering which successfully reproduces UCPLE spectra. This model also allows for deducing phonon energies and relative amplitudes of matrix element by fit to the UCPLE spectra. Additionally, our model accurately predicts the temperature dependence of UCPLE spectra. By clarifying the complexities of the upconversion phenomena in SWNTs, this study holds the potential to drive development in nanotube-based device applications.

Acknowledgements

This work is supported in part by JSPS (KAKENHI JP20H02558, JP23H00262 to Y.K.K., JP22H01893 to D.K.), and MEXT (ARIM JPMXP1222UT1136). We thank the Advanced Manufacturing Support Team at RIKEN for technical assistance.

References

[1] N. Akizuki, S. Aota, S. Mouri, K. Matsuda, and Y. Miyauchi, Nat. Commun. **6**, 8920 (2015).
[2] D. Kozawa, X. Wu, A. Ishii, J. Fortner, K. Otsuka, R. Xiang, T. Inoue, S. Maruyama, Y. Wang, and Y. K. Kato, Nat. Commun. 13, 2814 (2022).
[3] P. M. Vora, X. Tu, E. J. Mele, M. Zheng, and J. M. Kikkawa, Phys. Rev. B **81**, 155123 (2010).

Determination of in- and out-of-plane complex refractive index spectra of single-chirality carbon nanotube membranes

Hengkai Wu[1], Taishi Nishihara[1], Akira Takakura[1], Kazunari Matsuda[1], Takeshi Tanaka[2], Hiromichi Kataura[2], Yuhei Miyauchi[1]

[1] Institute of Advanced Energy, Kyoto University
[2] Nanomaterials Research Institute, National Institute of Advanced Industrial Science and Technology (AIST)
E-mail: wu.hengkai.68c@st.kyoto-u.ac.jp

Single-walled carbon nanotubes (SWCNTs) are promising opto-functional materials due to their strong light-matter interaction enabled by exciton states [1,2]. Since they are quasi-one-dimensional (1D) materials, they exhibit significantly different optical response to light with polarization parallel and perpendicular to the nanotube axis [3,4]. Recently, nanotube membranes with specific chiral structure (chirality) are promising for photonic [5] and opto-thermal applications [6] because the sharp and chirality-dependent excitonic resonance remains robust even at high temperature [6]. For the 1D feature of SWCNTs, their membranes which are 3D assemblies of SWCNTs with most of them oriented in the in-plane direction, are expected to exhibit anisotropic optical responses depending on the light propagating direction to the membrane plane. However, despite well-clarified response of an individual SWCNT, the anisotropic complex refractive index spectra of SWCNT membranes remain to be revealed yet, hindering prediction of angle-dependent optical responses and the design of SWCNT-based devices for the applications mentioned above.

Here, we report in- and out-of-plane complex refractive index spectra of a single-chirality SWCNT membrane, as examined using polarization- and angle-resolved reflection spectroscopy. The membrane was fabricated via the vacuum filtration of (6,5) SWCNT dispersion prepared using gel chromatography [5,7]. We measured the incident angle dependence of the reflectance spectra of *s*- and *p*-polarized light on the membrane in near-infrared-to-visible region (0.8–2.4 eV) using a homemade optical setup (Figure 1). We determined the in-plane complex refractive index spectrum from the reflectance of *s*-polarized light with different angles. The out-of-plane one is determined from the angle dependence of reflectance of *p*-polarized light, considering transverse exciton responses [3,4]. We found that the out-of-plane refractive index is almost constant (~1.9) in this region comparing to the wavy in-plane one, and the small contribution from the transverse exciton resonance is indispensable for properly predicting angle-dependent optical responses of the membrane. The complete knowledge on both in- and out-of-plane complex refractive index spectra of single-chirality SWCNT membrane facilitates the design of precise and diverse photonic and thermo-optic devices based on SWCNTs [8].

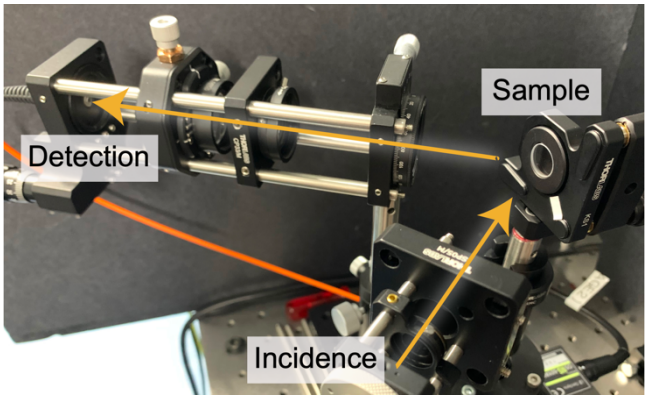

Figure 1: Homemade setup for incident angle-dependent reflectance measurement, consisted of an incidence part, a sample holder, and a detection part. The reflectance spectra at each angle are measured by changing the position of incidence and detection parts.

Acknowledgements

This work was supported by JST CREST Grant Number JPMJCR18I5, and JSPS KAKENHI Grant Number JP22K18287(Y.M.), JP19K15384(T.N.), JP21K14486(T.N.), and 23KJ1353(H.W.). This work was supported by Kyoto University Nano Technology Hub in “Nanotechnology Platform Project” sponsored by the Ministry of Education, Culture, Sports, Science and Technology (MEXT), Japan.

References

[1] T. Ando, J. Phys. Soc. Jpn. **66** (1997) 1066.
[2] F. Wang, G. Dukovic, L. E. Brus, T. F. Heinz, Science **308** (2005) 838.
[3] H. Ajiki, T. Ando, Phys. B: Condens. Matter **201** (1994) 349.
[4] Y. Miyauchi, M. Oba, S. Maruyama, Phys. Rev. B **74** (2006) 205440.
[5] T. Nishihara, A. Takakura, M. Shimasaki, K. Matsuda, T. Tanaka, H. Kataura, Y. Miyauchi, Nanophotonics **11** (2022) 1011.
[6] T. Nishihara, A. Takakura, Y. Miyauchi, K. Itami, Nat. Commun. **9** (2018) 3144.
[7] Y. Yomogida, T. Tanaka, M. Zhang, M. Yudasaka, X. Wei, H. Kataura, Nat. Commun. **7** (2016) 12056.
[8] H. Wu, T. Nishihara, A. Takakura, K. Matsuda, T. Tanaka, H. Kataura, Y. Miyauchi, *to be submitted*.

Changing from diffusive to superdiffusive transport in carbon nanotube networks via nematic order control

Filchito Renee G. Bagsican[1,2], Michael Wais[3,4], Natsumi Komatsu[5,6], Weilu Gao[7], Kazunori Serita[1], Hironaru Murakami[1], Karsten Held[4], Iwao Kawayama[1,8], Junichiro Kono[5,1,3], Marco Battiato[3], and Masayoshi Tonouchi[1]

[1]Osaka Univ., Japan, [2]FSU, OIST, Japan, [3]NTU, Singapore, [4]TU Wien, Austria, [5]Rice Univ., USA, [6]Univ. of California-Berkeley, USA, [7]Univ. of Utah, USA, [8]Kyoto Univ., Japan

E-mail: filchitorenee.bagsican@oist.jp

Carbon nanotubes (CNTs) exhibit extremely anisotropic electronic and optical properties due to the confinement of quasiparticles in one-dimension. This anisotropy disappears in an ensemble of randomly oriented CNTs, together with some other properties that make them attractive for certain device applications. However, it is unclear if this disorder suppresses other types of behaviors as well. In this work [1], we addressed this question by using a combination of terahertz (THz) emission and photocurrent experiments (Fig. 1a) with out-of-equilibrium numerical simulations to compare the dynamics of quasiparticles under strong electric fields in aligned and random CNT networks. We found that the degree of alignment has a strong influence on the dynamics and thermalization pathways of quasiparticles. In aligned CNTs, the electrons show superdiffusive transport properties and have a high probability of acquiring enough kinetic energy to produce low energy excitons via exciton impact ionization [2]. However, this process is significantly suppressed in random CNTs. Due to the increased impurity-like scatterings in random CNTs that arise from multiple tube distortions in the intersecting tubes, the electrons show diffusive transport properties and do not gain the kinetic energy required for exciton impact ionization. This difference in electron transport regimes (superdiffusive vs diffusive) leads to drastically different bias-dependence of THz emission amplitude and photocurrent in aligned and random CNT networks as shown in Figs. 1b and 1c, respectively.

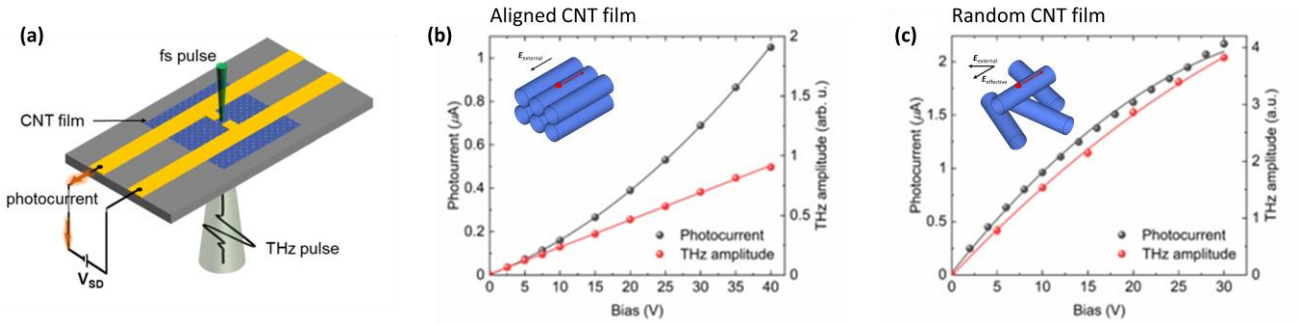

Fig. 1. Device configuration (a). Terahertz emission amplitude and photocurrent as a function of bias for aligned (b) and random (b) CNT films. Adapted from [1].

Acknowledgements

This work is supported by Robert A. Welch Foundation (C-1509), Air Force Office of Scientific Research (FA9550-22-1-0382), JST CREST (JPMJCR17I5 and JPMJCR22O2), US National Science Foundation (PIRE-2230727), Carbon Hub of Rice University, Nanyang Technological University (NAP-SUG), Austrian Science Fund (P36213 and Doctoral School W1243 Solids4Fun (Building Solids for Function)), JSPS KAKENHI (JP18KK0140, JP23H00184, and JP22H01550), JSPS Core-to-Core Program, Osaka University Program for Promoting International Joint Research and Iketani Science and Technology Foundation.

References

[1] Wais, M., *et. al*, Nano Lett. 23, 10 (2023) 4448–4455.
[2] Bagsican, F.R.G., *et. al*, Nano Lett. 20, 5 (2020) 3098–3105.

Plasmonic rectification effect in an asymmetric periodically gated graphene field effect transistor for THz detection

Chao Tang[1,2], Hironobu Seki[1,3], Koichi Tamura[1,3], Shinnosuke Uchigasaki[1,3], Hirokazu Fukidome[1], Yuma Takida[4], Hiroaki Minamide[4], Akira Satou[1] and Taiichi Otsuji[1]
[1] Research Institute of Electrical Communication, Tohoku University [2] Frontier Research Institute for Interdisciplinary Sciences, Tohoku University [3] School of Engineering, Tohoku University [4] RIKEN Center for Advanced Photonics, RIKEN
E-mail: tang.chao.c4@tohoku.ac.jp

1. Introduction

In this study, we propose a novel approach to THz wave detection using an asymmetrically gated graphene field-effect transistor (GFET). By utilizing two sets of gates arranged in an asymmetric manner, we achieve periodic modulation of the carrier density along the channel. Previous research has explored various mechanisms for THz detection, including the photo-thermalelectric (PTE) effect, photovoltaic (PV) effect, bolometric (BM) effect, and plasma rectification (PR) [1]. While PR [2] has been observed in a direct-current photoresponse [3], but yet to be in fast temporal response. Our study aims to provide direct evidence of PR-based fast-speed detection in a GFET. We apply a specific bias to the asymmetrically gated GFET, resulting in a periodically arranged carrier density and observing clear evidence of PR in the graphene channel.

2. Experiments and results

We fabricated the GFET using similar methods as described in a previous publication [4], but with the use of ALD for the dielectric layer instead of CVD (Fig. 1a). THz pulse detection measurements were conducted on the fabricated GFET using an injection-seeded THz parametric generator (is-TPG) [5] as the pulsed-CW THz light source. The THz pulse had a center frequency of 0.95 THz and an envelope pulse width of 155 ps. To verify the detection of plasma rectification along the channel, we set the bias of the source and drain electrodes to 0 V. Additionally, we ensured that the same metal type was used for both the source and drain electrodes, eliminating any potential gradient along the graphene channel. As a result, even if the channel carriers were excited by THz radiation, no photoresponse could be promoted through the PTE or PV effects. Fig. 1b shows the photovoltage detected from the source and drain under different G1-G2 bias conditions. The charge neutral point voltage (V_{CNP}) was identified to be +4 V by the ambipolar characteristics (Fig. 1b inset). During the THz detection experiments, we applied a bias of −10 V to the G1 electrode (V_{G1}) to introduce holes into the channel. Simultaneously, we varied the bias of V_{G2} to −10, 0, +4, and +10 V.

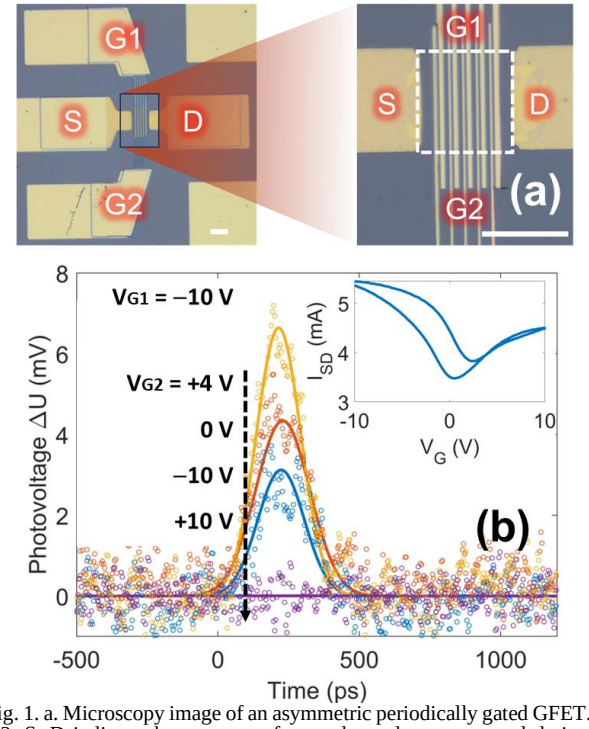

Fig. 1. a. Microscopy image of an asymmetric periodically gated GFET. G1, G2, S, D indicate the two sets of gate electrodes, source and drain gate, respectively. The dashed line indicates the graphene channel region. (Scale bar: 20 μm) b. The photovoltage response of the device to THz radiation. The time = 0 ps represents the start of radiation on the GFET.

Our observations indicate that when carriers of different types are injected into the region beneath G2 (V_{G2}=10V), no photovoltage is generated in response to THz radiation. This can be attributed to the recombination of holes underneath G1 with the electrons underneath G2, preventing carriers from reaching the drain electrode and generating a photovoltage. On the other hand, when carriers of the same type but with different densities (−10 V, 0 V, 4 V) are injected, fast photoresponse was observed thanks to the PR mechanism (Fig. 1b). This phenomenon cannot be solely explained by the PTE or PV effect, as no bias was applied to the source and drain electrodes, thereby eliminating any potential gradient that could drive photo-excited carriers from the source to the drain electrode. Moreover, the photovoltage reaches its maximum when G2 is depleted, and it increases as the difference in carrier density between G1 and G2 becomes larger. These phenomena can be attributed to the PR effect [6].

3. Conclusion

Our study demonstrates that by adjusting the carrier distribution in the channel through the biasing of G1 and G2, without applying any bias to the source and drain electrodes, the detection of THz radiation can be achieved through plasmonic rectification. This highlights the potential of using an asymmetric periodically gated GFET for THz detection based on plasmonic effects.

Acknowledgments: A part of this work was financially supported by RIEC Tohoku University, FRIS, Tohoku University, also support by The Japan Society for Promotion of Science KAKENHI Grants #21H04546, #22KF0430, and the Commissioned Research by NICT #01301, Japan.

References

[1] F.H. Koppens, et. al., *Nat. Nanotechnol*. **9** (2014) 780.
[2] M. Dyakonov, M. Shur, *IEEE Trans. Elec. Dev*. **43**, (1996) 3.
[3] J.A. Delgado-Notario et al., *Nanophoton.* **11**, (2022) 519.
[4] K. Tamura, et. al. *APL Photon*. **7** (2022) 126101.
[5] Y. Takida, et. al. *Opt. Exp.* **30** (2022) 11217.
[6] V.V. Popov, *Appl. Phys. Lett.* **102** (2013) 253504.

Moiré excitonic states in a twisted $WSe_2/MoSe_2$ heterobilayer

Keisuke Shinokita
Institute of Advanced Energy, Kyoto University

E-mail: shinokita.keisuke.4r@kyoto-u.ac.jp

1. Introduction

Atomically thin transition metal dichalcogenides (TMDs) are considered ideal two-dimensional systems with intriguing optical properties associated with valley degrees of freedom [1]. Van der Waals heterostructures composed of TMDs provide a fascinating platform for engineering optically generated excitonic properties through moiré patterns, which arise from the angular mismatch, leading to novel quantum phenomena. The periodic trap potential of the moiré pattern enables the formation of spatially ordered ensembles of zero-dimensional excitons, known as moiré excitons. These excitons offer the potential for dense coherent quantum emitters and quantum simulation of many-body physics [2]. In this study, we present the characterization of excitonic states within the moiré potential in a twisted $WSe_2/MoSe_2$ heterolayer.

2. Results and Discussion

Figure 1(a) shows the optical microscopy image of the $WSe_2/MoSe_2$ heterobilayers. The twist angle of the heterobilayers is 12±1°. Figure 1(b) displays the photoluminescence (PL) spectra at 10 K. Several distinct peaks in the PL spectra, characterized by a linewidth of approximately 0.6 meV, signify the response of zero-dimensional interlayer excitons trapped within the moiré potential, known as moiré excitons.

Figure 1(c) depicts counterplots of photoluminescence excitation (PLE) spectra. The resonance behavior is clearly illustrated in the 2D color map of excitonic emissions shown in Figure 1b, representing the dependence on excess energy. Notably, the emission of moiré excitons is enhanced when excited with excess energies of approximately 24 and 48 meV, indicating an interaction between the moiré excitons and phonons. Conversely, the PL intensities significantly decrease under off-resonance conditions, suggesting the existence of discrete energy levels for excitons within the moiré potential [3].

In Figure 1(d), circularly polarized photoluminescence (PL) spectra are presented under σ^+ excitation. The optical selection rule of the valley-polarized moiré excitons causes the σ^- emission stronger than the σ^+ emission, resulting in negative circular polarization. Moreover, the σ^- emission experiences resonant enhancement when subjected to σ^+ excitation with an excess energy of approximately 24 meV, while the σ^+ emission remains unaffected. This observation suggests the resonant excitation of a spin-triplet state with σ^+ excitation, followed by relaxation to a spin-singlet state accompanied by the emission of a chiral phonon, resulting in σ^- emission from the spin-singlet state. This behavior reflects the fine structure of excitons within the moiré potential [4].

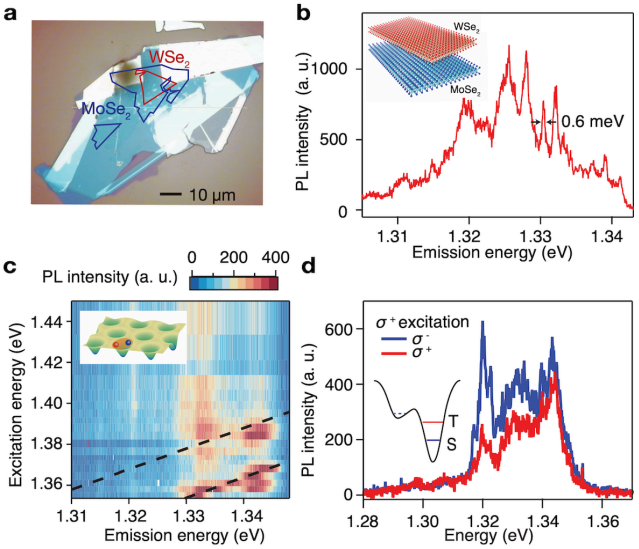

Fig. 1. (a) Optical microscopy image of a twisted $WSe_2/MoSe_2$ heterobilayer. (b) Photoluminescence (PL) spectrum at 10 K. (c) 2D color map showing the PL intensity as a function of excitation energy. The black dashed line indicates excess energies of 24 and 48 meV. (d) Circularly polarized PL spectra under σ^+ excitation. The inset depicts the fine structures of the moiré excitons.

3. Conclusions

The excitonic states within a moiré potential were examined in a twisted $WSe_2/MoSe_2$ heterobilayer. Photoluminescence excitation (PLE) spectroscopy revealed the discrete energy levels present within the moiré potential. Furthermore, circularly-polarized photoluminescence (PL) spectroscopy provided insights into the fine structures of the moiré excitons.

Reference

[1] K. Shinokita *et al.*, Adv. Funct. Mater. **29**, 190260 (2019).
[2] K. L. Seyler *et al.*, Nature **567**, 66 (2019).
[3] K. Shinokita *et al.*, Nano Lett. **21**, 5938 (2021).
[4] K. Shinokita *et al.*, ACS Nano **16**, 16862 (2022).

Remote charge modulation effect of monolayer MoS_2 using periodically polarization-inverted structure and hBN spacer layer

Ritsumeikan Univ. [1], Osaka Univ.[2], Kyoto Univ.[3], Kaipeng Rong[1], Ryosuke Noro[2], Hayato Nishigaki[2], Mingda Ding[2], Yao Yao[2], Taiki Inoue[2], Ryuji Katayama[2], Yoshihiro Kobayashi[2], Kazunari Matsuda[3], ◦Shinichiro Mouri[1]

E-mail: gr0466er@ed.ritsumei.ac.jp

Molybdenum disulfide (MoS_2) is a typical two-dimensional layered material that exhibits unique properties offering opportunities for the development of nanoelectronics, valleytronics, and spintronics. Exploring the way to modulate carrier distribution is an important issue for controlling these device performance [1]. Here we demonstrate the "remote" spatial carrier modulation method for MoS_2 using periodically polarization inversed ferroelectric structure and spacer h-BN layers.

We transferred exfoliated few layers hBN and monolayer MoS_2 flake sequentially onto a periodically polarization-inverted structure formed on a ferroelectric substrate MgO: $LiNbO_3$. The schematic cross-sectional image of the sample was shown in upper of Fig.1. Photoluminescence (PL) mapping measurement was carried to investigate the distribution of charge density of monolayer MoS_2. Lower of Fig. 1 shows the PL mapping image of this sample, expressing the intensity ratio of trion peak (I_T, ~1.84eV) and exciton peak (I_X, ~1.88 eV), which changes according to the charge density. It clearly shows that the exciton weight of monolayer MoS_2 changes spatially, depending on the polarization of substrate. We also plot the I_T/I_X value in Fig.1(b) along the line shown in Fig 1 (a). It shows that the value of I_T/I_X approximately equals 0.5 and 2 relatively on down- and up-domain.

These results indicate that electron density is larger on up-domain region as compared with down-domain region. Rough estimation using Saha equation[2] provides that the carrier density on up domain is about 4 times larger than that on down domain. It is note that the strong polarization effects of ferroelectric substrate remains even through the existence of few layer h-BN. There could be two possibilities to account this "remote" spatial carrier modulation as following. The tunneling charge transfer through h-BN layer via impulity states is one possible mechanism. Another is the strong surface electric field move charge carriers directly resulting in the redistribution. Detail model will be discussed in the presentation.

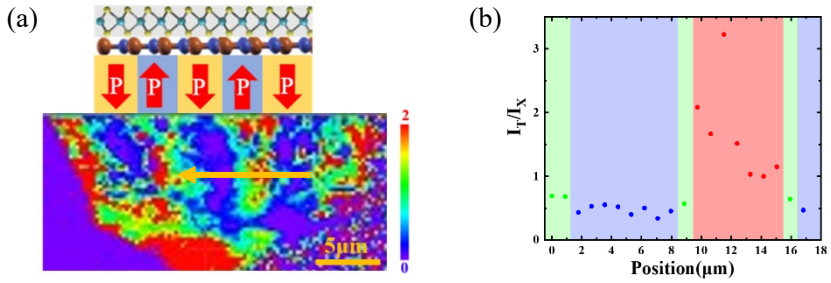

Fig.1 (a) Cross-sectional diagram of the sample and PL intensity ratio (I_T/I_x) mapping
(b) The change of PL intensity ratio along the line in Fig.1 (a).

[1] X. Wang *et al.*, Adv. Mater. **27**, 6575-6581(2015).
[2] S. Mouri *et al.*, Nano Lett. **13** (12), 5944-5948 (2013).

This work was supported by JSPS KAKENHI grant number 22H05471, 21H01017, 21K18913, and NEDO "Intensive Support Program for Young Promising Researchers"

Observation of quantum coherence of a single moiré exciton in nano-fabricated twisted $MoSe_2/WSe_2$ heterobilayers

Haonan Wang[1], Heejun Kim[1], Duanfei Dong[1], Keisuke Shinokita[1], Kenji Watanabe[2], Takashi Taniguchi[3] and Kazunari Matsuda[1]

[1]Institute of Advanced Energy, Kyoto University, [2]Research Center for Electronic and Optical Materials, NIMS, [3]Research Center for Materials Nanoarchitectonics, NIMS
E-mail: wang.haonan.36t@st.kyoto-u.ac.jp

1. Introduction

Recently, rapid progress on artificial van der Waals (vdW) structures by stacking atomically thin two-dimensional materials has opened up new opportunities for the design of novel quantum systems [1]. Three-dimensional confinement provided by the periodic ordered potential traps not only makes moiré system promising for achieving long coherence time [2], but also suitable for exploring interaction between systems. However, broad emissions attributed to ensemble-averaged multiple peaks caused by inhomogeneity of the moiré potentials hinder the detail exploration of quantum coherence and interference of the moiré system.

2. Results

In this study, we have developed and applied a new strategy of nano-fabrication to observe quantum coherence and interference of a single moiré exciton in $MoSe_2/WSe_2$ vdW heterobilayers beyond the diffraction limit of light. A significant single and sharp photoluminescence (PL) peak from single moiré exciton has been successfully demonstrated by applying reactive-ion-etching to the heterobilayer, as presented in **Figure 1**. With further increasing the excitation powers, the single and sharp PL shows the saturation behaviors. We further investigate the duration of quantum coherence of the single moiré exciton, which reaches beyond 10 ps as well as the accelerated decoherence process with elevating temperature and excitation power density. Moreover, the significant quantum interference indicated by quantum beats from temporal interferogram has revealed the coupling between moiré excitons trapped in different moiré potential minima.

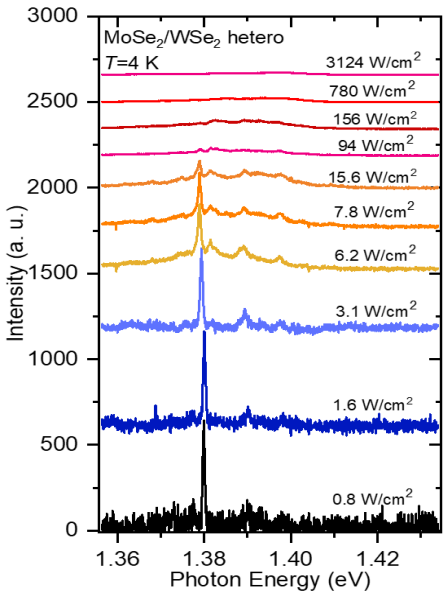

Figure 1 Normalized photoluminescence spectra of $MoSe_2/WSe_2$ heterobilayer under excitation of various power densities.

3. Conclusions

A new method to realize the optical observation of quantum coherence and interference of single moiré exciton has been demonstrated, which will facilitate potential application toward quantum technologies based on moiré quantum systems.

References

[1] K.L. Seyler. et al. *Nature.* **567**, 66–70 (2019).
[2] U. Hendrik.et al. *Science* **363**,1068-1072 (2019).

Chemically-tailored semiconductor moiré superlattices

Wenjin Zhang[1], Zheng Liu[2], Hiroshi Nakajo[3,4,5], Soma Aoki[3,4], Haonan Wan[6], Yanlin Wang[6], Yanlin Gao[7], Mina Maruyama[7], Takuto Kawakami[8], Yasuyuki Makino[1], Masahiko Kaneda[1], Tongmin Chen[9], Kohei Aso[9], Tomoya Ogawa[1], Takahiko Endo[1], Yusuke Nakanishi[1], Kenji Watanabe[10], Takashi Taniguchi[11], Yoshifumi Oshima[9], Yukiko Yamada-Takamura[9], Mikito Koshino[8], Susumu Okada[7], Kazunari Matsuda[6,] Toshiaki Kato[3,4], and Yasumitsu Miyata[1]

[1] Department of Physics, Tokyo Metropolitan University, Hachioji 192-0397, Japan; [2] Innovative Functional Materials Research Institute, National Institute of Advanced Industrial Science and Technology (AIST), Nagoya 463-8560, Japan; [3] Graduate School of Engineering, Tohoku University, Sendai, 980-8579, Japan [4] Advanced Institute for Materials Research (AIMR), Tohoku University, Sendai, 980-8577, Japan; [5.] KOKUSAI ELECTRIC CORP., Toyama 939-2393, Japan; [6] Institute of Advanced Energy, Kyoto University, Kyoto, 611-0011 Japan; [7] Department of Physics, Graduate School of Pure and Applied Sciences, University of Tsukuba, Tsukuba 305-8571, Japan; [8] Department of Physics, Osaka University, Toyonaka, Osaka 560-0043, Japan; [9] School of Materials Science, Japan Advanced Institute of Science and Technology (JAIST), Ishikawa 923-1292, Japan; [10] Research Center for Electronic and Optical Materials, NIMS, Tsukuba 305-0044, Japan; [11] Research Center for Materials Nanoarchitectonics, NIMS, Tsukuba 305-0044, Japan;
E-mail: ymiyata@tmu.ac.jp; kato12@tohoku.ac.jp and wjzhang@tmu.ac.jp

Introduction

The nanoscale periodic potential generated from moiré superlattices provides a new knob to tune and study the flat band effect and correlated physics. To date, moiré superlattices have been obtained using various two-dimensional (2D) materials, such as graphene, hexagonal boron nitride (hBN), transition metal dichalcogenides (TMDCs), and so on. In the 2D materials family, Janus monolayers of TMDCs have two different chalcogen atoms above and below the central metal atom. This asymmetric structure induced an out-of-plane electric field which provides an additional degree of freedom in moiré superlattices. Novel features in Janus materials were predicted by recent theoretical studies, such as: large Rashba spin–orbit coupling[1], piezoelectricity[2], and long-lived charge-transfer excitons[3]. Furthermore, recent calculations showed that excitons in Janus heterobilayer moiré superlattices are possible to realize high-temperature Bose–Einstein condensation state[3].

Although Janus TMDC monolayers and heterobilayers were obtained using thermal or plasma-assisted chemical reactions and transfer process[4,5], the experimental evidence of moiré superlattice and related excitonic properties in Janus heterobilayers are still unknown. Importantly, the small lattice mismatch between MX_2 and MXY enables the formation of long-wavelength moiré superlattices, even from non-twisted bilayers in Janus heterobilayers. Therefore, direct preparation of Janus heterobilayers provides a scalable method for making moiré superlattices from MX_2 bilayers. Here, we show experimental evidence for the formation of moiré superlattices and the associated excitonic responses in Janus heterobilayers of MoSSe/$MoSe_2$ and WSSe/WSe_2.

Figure 1a shows the schematic of Janus MoSSe/$MoSe_2$ moiré superlattice fabricated from bilayer $MoSe_2$ using plasma-assisted chemical reactions. After the plasma treatment, moiré pattern was generated because of the mismatch of lattice constant between MoSSe and $MoSe_2$. Figure 1b shows the photoluminescence (PL) spectrum at cryogenic temperature. The sharp PL peaks representing moiré potential trapped exciton emissions were observed. This gives an evidence of successful fabrication of moiré superlattice.

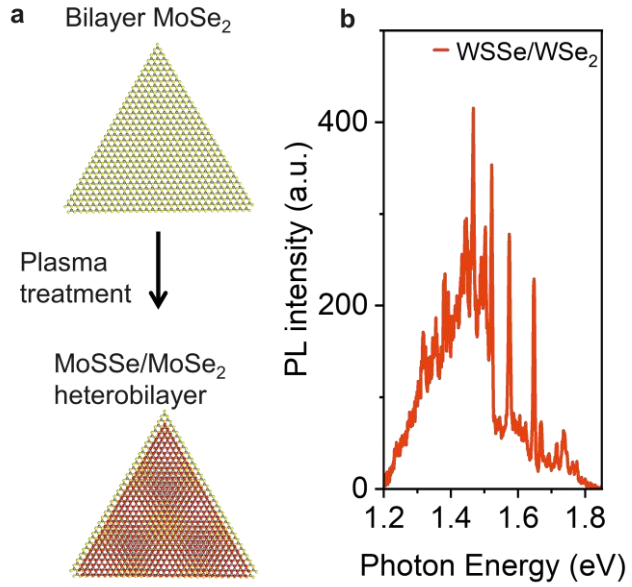

Figre 1. (a) Schematic of moiré superlattice fabricated from bilayer TMDC using plasma assisted chemical reactions. (b) PL spectrum of Janus heterobilayer WSSe/WSe_2 at 8 K.

References

[1] Q.-F. Yao, et al., Phys. Rev. B 2017, 95, 165401.
[2] L. Dong, et al., ACS Nano 2017, 11, 8242.
[3] H. Guo, et al., Sci. Adv. 2022, 8, eabp9757.
[4] A.-Y. Lu, et al., Nat. Nanotechnol. 2017, 12, 744.
[5] D. B. Trivedi, et al., Adv. Mater. 2020, 32, 2006320.